Dyes and Pigments 150 (2018) 301–305

Contents lists available at ScienceDirect

Dyes and Pigments

journal homepage: www.elsevier.com/locate/dyepig

A novel dual-emitting luminescent metal-organic framework for naked-eye and microgram detection of picric acid

Jian Wang*, Lingwen Zhang, Liang Bao, Li Zhou, Yangying Liu, Pengyan Wu**

School of Chemistry and Materials Science & Jiangsu Key Laboratory of Green Synthetic Chemistry for Functional Materials, Jiangsu Normal University, Xuzhou, Jiangsu, 221116, China

ARTICLE INFO

Keywords:
Metal-organic frameworks
Picric acid
Dual-emitting
Luminescent sensor
Naked-eye

ABSTRACT

Picric Acid (PA) is directly associated with modern bombs in terrorist attacks or other criminal intents, thus, a simple yet sophisticated bi-signal emission system based on MOFs is one of the breakthroughs to increase the accuracy and sensitivity for PA detection. Herein, ligand-to-metal charge-transfer (LMCT) related emission and the ligand-based emission were formed simultaneously within a novel luminescent MOF with a 2D pore system, which was constructed by choosing d^{10}-metal Zn(II) as nodes and luminescent organic ligand 9-phenylcarbazole-3,6-dicarboxylic acid (H_2PDA) as linkers. It can serve as the first example of MOFs implicated dual-emitting sensor for visual and selective luminescent sensing of PA. The naked-eye and luminescent detection limitations for PA are 0.45 *μg* and 25 *ppb*, respectively, and it could be regenerated by hot ethanol treatment and reused at least for 5 times. The sensing mechanism is also discussed through IR, ^{1}H NMR and molecular force field-based calculations.

1. Introduction

As it is well-known that there are potentially disastrous problems related to environmental pollution in the world, so that the development of methods to cope and resolve those problems has been a formidable challenge for engineers, environmentalist and chemists, and other related interdisciplinary scholar [1]. One of the main concern of environmental pollutant is the hidden nitrated aromatic explosives, because of its direct correlation with modern bombs in criminal intents or terrorist attacks and its intense irritation to the eye/skin, as well as its potential damage to the respiratory system [2,3]. Recently, a lot of instrumental techniques are used to detect explosives, *e.g.* 2,4,6-trinitrotoluene (TNT), picric acid (PA) and 2,4-dinitrotoluene (DNT), which are the primary components of lots of unexploded land mines around the world [4–6]. Among these methods, fluorescence quenching based explosives detection has grown drastically on account of its easy visualization, high sensitivity, fast response and real-time monitoring [7–9]. And the main detection mechanism is the photo-induced donor–acceptor electron transfer (PET) from the excited host to explosives, however, the selective sensing of PA over other explosives still remains a challenge due to the similarity of their structures [10–12]. Its intrinsic hydroxyl group besides from the electron deficient nitro group as the potential hydrogen bonding donor-acceptor is vital for the detection of PA related explosives.

Metal−organic frameworks (MOFs), as a kind of new crystalline porous materials, formed by metal ions (or clusters) as the joints and multi-directional organic ligands as bridgings have gained extensive concerns due to their designed structures in addition to their wide applications in optical sensing/detection [13–17], gas storage and separation [18–21], drug delivery [22,23], catalysis [24–26], and magnetic materials [27,28]. Luminescent MOFs (LMOFs) are promising candidates for recognition application based on their ability to easily transform the host–guest interaction into determinable luminescence changes. The introduction of metal nodes and organic linkers with high conjugacy as well as the adjustable pores within the well-organized framework not only permits various variation of fluorescence emissions through tuning different parameters, *e.g.* organic linkers, metal ions, or metal-organic charge-transfer, but also can lead to the host–guest interaction enhancement by many folds. Although there are lots of LMOFs has been reported for explosives detection, sensing functionality in most of LMOFs is fulfilled based on mono-signal emission, which is generally blue- or red-shifted in the emission peak derived from photo-induced electron transfer between the excited host and explosives, leading to difficulty in quantification [29–31]. A simple yet sophisticated bi-signal emission system based on MOFs is one of the breakthroughs to increase the accuracy and sensitivity for explosives detection. Since the charge-transfer luminescence is normalcy found in d^{10} metal-based MOFs [13,32–34], and

* Corresponding author.
** Corresponding author.
E-mail addresses: wjian@jsnu.edu.cn (J. Wang), wpyan@jsnu.edu.cn (P. Wu).

https://doi.org/10.1016/j.dyepig.2017.12.032
Received 4 September 2017; Received in revised form 6 November 2017; Accepted 16 December 2017
Available online 18 December 2017
0143-7208/

sometimes, charge-transfer luminescence may compete with luminescence based on the ligands, thereby generating two emission bands, herein, we reported a dual-emitting 3D MOFs, $\{[Zn_4O(C_{20}H_{11}NO_4)_3(C_4H_9NO)(H_2O)]\cdot(C_4H_9NO)_2(H_2O)_3\}_n$ (Zn−PDA2) including metal ligand charge-transfer related emission and the ligand-based emission. And the sensing of explosives was studied in detail.

2. Experimental

2.1. Methods and measurements

All chemicals with reagent grade quality were gained from commercial sources. 4-Aminophenol was purchased from J&K Scientific, Picric Acid and the other nitroaromatics were provided from Xiya Reagent Company (China). 9-Phenylcarbazole was purchased from Qingdao Frontierchem Co., Ltd.. Instruments and spectroscopic measurements: The C, H and N elemental analyses were determined on a Vario EL III elemental analyzer. ^{1}H NMR spectra were tested on a Bruker-400 spectrometer with Me_4Si as an internal standard. X-Ray powder diffraction (XRD) patterns of the Zn−PDA2 was recorded on a Rigaku D/max-2400 X−ray powder diffractometer (Japan) using Cu−Kα (λ = 1.5405 Å) radiation. Thermogravimetric analysis (TGA) was collected in a nitrogen flow of a Mettler-Toledo TGA/SDTA851 instrument at a 5 °C/min ramp rate. FT-IR spectra were carried out on Bruker Optics TENSOR 27 FT-IR spectrophotometer using KBr pellets. Solid ultraviolet–visible spectra were obtained on a HP 8453 spectrometer. Fluorescent spectra of the solution were measured on Hitachi F-4600. Fluorescence measurements of Zn−PDA2 suspension were performed in a 1 cm quartzcuvette, the emission and excitation slit widths were both 2.5 nm. For nitro-aromatic molecular detection, the solutions of related nitro-analysts with 2.0×10^{-2} M concentration were prepared in ethanol.

2.2. Synthesis of the H_2PDA ligand

(a) Synthesis of 3,6-diacetyl 9-phenylcarbazole.

To the solution of 9-phenylcarbazole (2.0 g, 8.2 mmol) and 2.4 g (18.0 mmol) $AlCl_3$ in 100 mL dry CH_2Cl_2, 2.7 mL (28.28 mmol) acetyl chloride in 30 mL dry CH_2Cl_2 was added dropwisely. Then the reaction was carried out at room temperature for 12 h and 100 mL water was added. The aqueous layer was further extracted with CH_2Cl_2 (3 × 150 mL); the combined organic layers were dried by Na_2SO_4. The solution was concentrated under reduced pressure to give the crude product, which was purified by flash column chromatography on silica gel (1: 10 hexanes–CH_2Cl_2) to afford a yellow solid (1.46 g, 54.3%). ^{1}H NMR ($CDCl_3$, *ppm*): δ 9.16 (s, $2H_{Ar}$), 8.08 (d, J = 8.0 Hz, $2H_{Ar}$), 7.73 (d, J = 8.0 Hz, $2H_{Ar}$), 7.67–7.61 (m, $3H_{Ar}$), 7.42 (d, J = 8.0 Hz, $2H_{Ar}$), 2.72 (s, $6H_{-COCH3}$).

(b) Synthesis of 9-phenylcarbazole-3,6-dicarboxylic acid.

3 mL Br_2 were added dropwisely to the solution of NaOH (7 g, 0.18 mol) in 30 mL water on ice-bath, and further stirred for 20 min. The solution were dumpage to a isobarically funnel and were added dropwisely to a solution of 3,6-diacetyl 9-phenylcarbazole (1.2 g, 3.6 mmol) in 30 mL 1,4-Dioxane on 45 °C during 5 h. Then the mixture was put on ice-bath, saturated hydroxylamine HCl was added to deoxidize excessive sub-bromo-sodium. The solution was acidified by muriatic acid and the solid product was filtered and dried under vacuum. The crude was recrystallized from acetic acid to afford pure products as a white solid. (1.0 g, 84.5%). ^{1}H NMR (DMSO-d6, *ppm*): δ 12.84 (s, $2H_{COOH}$), 9.0 (s, $2H_{Ar}$), 8.10 (d, J = 8.0 Hz, $2H_{Ar}$), 7.76–7.63 (m, $5H_{Ar}$), 7.44 (d, J = 8.0 Hz, $2H_{Ar}$). ^{13}C NMR (DMSO-d6, *ppm*): δ 167.7 (C_{COOH}), 143.5 (C_{Ar}), 135.9 (C_{Ar}), 130.5 (C_{Ar}), 128.7 (C_{Ar}), 128.3 (C_{Ar}), 127.1 (C_{Ar}), 123.6 (C_{Ar}), 123.0 (C_{Ar}), 122.5 (C_{Ar}), 109.9 (C_{Ar}). Anal calc. for $C_{20}H_{13}NO_4$: C 72.50, H 3.95, N 4.23%; Found: C 72.52, H 3.94, N 4.22%. TOF MS calcd for $C_{20}H_{13}NO_4$ 331.32, found 331.41.

2.3. Synthesis of Zn−PDA2

A mixture of 9-phenylcarbazole-3,6-dicarboxylic acid (H_2PDA) (17 mg, 27 mM), $Zn(NO_3)_2\cdot6H_2O$ (75 mg, 125 mM) and 15 μL TEA were dissolved in dimethylacetamide/water (9/1, 5 mL) in a screw capped vial. The resulting mixture was placed in an oven at 120 °C for 3 days. Colorless crystals with block-shape were obtained after filtration. Yield: 80%. Anal calc. for $C_{72}H_{68}N6O_{20}Zn_4$: C 54.08, H 4.29, N 5.26%; Found: C 53.94, H 4.23, N 5.22%.

3. Results and discussion

3.1. Crystal description

The interdigitated structures Zn−PDA2 were prepared *via* hydrothermal reactive crystallization of $Zn(NO_3)_2\cdot6H_2O$ and efficient electron-donating bridging di-carboxylate H_2PDA (9-phenylcarbazole-3,6-dicarboxylic acid). X-ray analysis displayed Zn−PDA2 crystallize in the monoclinic crystal with space group $P2(1)/n$. There are one $Zn_4(\mu_4$-O) cluster, three PDA^{2-} ligands, one DMF, one water molecule and two free DMF and one free water molecules in an asymmetric unit. The Zn_4O SBUs are encapsulated by six carboxylate groups from six PDA^{2-} ligands to generate an interesting 3D microporous framework (Scheme 1). It has a two-dimensional (2D) pore system parallel to *ac*-plane consisting of 1D 10.4 × 13.6 $Å^2$ elliptical channels along the *a*-axis and smaller channels of 8.3 × 12.2 $Å^2$ along the *c*-axis present within the 3D non-interpenetrating extended network and 48.8% of solvent-accessible volume (4586.2 $Å^3$; calculated by the PLATON program), thus allowing the ingress and egress of the aromatic nitro-explosives in and out of Zn−PDA2.

3.2. Fluorescent properties and sensing of PA

Solid ultraviolet–visible spectrum of Zn−PDA2 showed an absorption band appeared around 326 nm, which belonged to the 9-phenylcarbazole moieties [35]. Zn−PDA2 ethanol suspension not only reveals an emission at 366 nm when excitated at 326 nm, which can be assignable to the intraligand charge transfer (ILCT) because similar

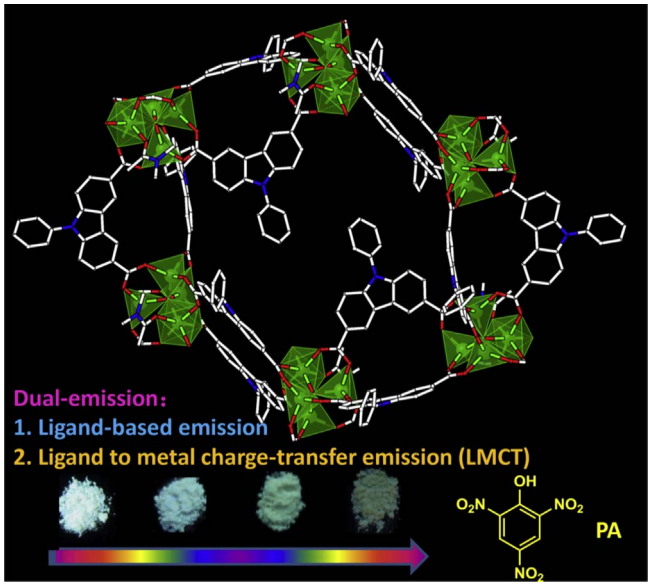

Scheme 1. The crystal packing diagram of Zn−PDA2 along *c*-axis with the ellipsoid cavities, constructed by H_2PDA ligands and "Naked-eye" luminescence recognition process between Zn–PDA2 and PA.